Stochastic resonance using noise generated by a neural network

G. Mato
Comisión Nacional de Energía Atómica and CONICET, Centro Atómico Bariloche and Instituto Balseiro (CNEA and UNC), 8400 San Carlos de Bariloche (RN), Argentina

(Received 25 August 1998; revised manuscript received 9 October 1998)

We study the phenomenon of stochastic resonance when the noise is generated by a network of integrate-and-fire neurons. A network with two populations of neurons (one excitatory and one inhibitory) and a dispersion of intrinsic firing rates can display a great amount of variability and its output can be used to improve the signal-to-noise ratio of another neuron that is receiving a subthreshold signal. We compare the performance of this system to that of a system using white noise with different distributions. We find network parameters for which the performance is similar to that of a system receiving white noise. In other cases, when the network output displays an oscillatory component, the signal-to-noise ratio has several peaks, We also analyze the relation between the synchrony of the network and the signal-to-noise ratio.
[S1063-651X(99)11502-2]

PACS number(s): 87.10.+e, 05.40.Ca, 02.50.Fz

I. INTRODUCTION

Stochastic resonance (SR) is a phenomenon first described in the context of bistable systems. Such a system upon receiving a small periodic signal will be always trapped in one of the minima if the signal is not strong enough to overcome the potential barrier. On the other hand, if a noisy input is also present the passage will be facilitated. This gives rise to the apparently paradoxical effect that signal detection can be facilitated by a suitable level of noise. This idea has been applied to explain the recurrence of Earth's ice ages [1,2], and later applied to a variety of systems such as electronic circuits, lasers, superconducting devices, single potential wells, individual neurons, and neural networks [3–8].

The phenomenon has obvious implications for information processing in the nervous system, as it could enhance signal detection. It has been experimentally observed in several systems, such as mechanoreceptive neurons in the crayfish [3,9], rat skin [10], and neurons in mammal brain [11]. One of the most interesting features of these experiments is that even when there is no *external* noise the system can detect the periodic signal (although the introduction of external noise can still improve the performance). This suggests that there might be an *internal* source of noise. Brain activity displays a great amount of variability, although its origins are not completely clear [12]. This variability could be used as the source of noise for implementing SR. A first analysis of this situation was carried out in [13] where the output of a network of Hindmarsh-Rose neurons was used to enhance a weak periodic signal. There it was shown that, effectively, noise generated by a network can improve signal detection.

Improving the performance of biological systems implementing SR has proved to be quite difficult. For instance, in the crayfish it has been shown that raising the temperature fails to show optimization as a function of the noise level [14]. Noise generated by a network has the potential advantage that its properties could be easily modified by tuning the network parameters. In this work we address the question of the relation between the dynamical state of a network and the phenomenon of SR when the output of the network is used as the noisy part of the input. To do this we simulate an integrate-and-fire (IF) network with two populations of neurons (one excitatory and one inhibitory) and a dispersion of intrinsic firing rates. This kind of network is able to generate an irregular pattern of activity, the characteristics of which can be controlled by changing the internal coupling constants. The paper is organized in the following way: in the next section we introduce the model for the network and the ''target'' neuron that receives a periodic signal. In Sec. III we introduce the parameters that characterize the dynamical state of the network and show the simulation results. We also compare these results with simulations that use white noise. In the last section we discuss the results.

II. MODEL

The model has two parts. The first is a network of N IF neurons that generate the noisy input for the additional target neuron that also receives a subthreshold periodic signal. The network has N_e excitatory neurons and N_i inhibitory neurons. The subthreshold dynamics of neuron j in the excitatory population is given by [15]

$$\tau \frac{dV_j}{dt} = -V_j(t) + I_j + G_{ee}(t)[V_e - V_j(t)] + G_{ie}(t)[V_i - V_j(t)], \quad (1)$$

where $V_j(t)$ is the membrane potential, τ is the membrane time constant, I_j is the bias current that controls the firing rate in the absence of interaction, and V_e and V_i are, respectively, the reversal potential of the excitatory and inhibitory interactions. The synaptic conductances $G_{ee}(t)$ and G_{ie} represent the interactions whithin the excitatory population and from the inhibitory population to the excitatory one, respectively. Similarly the dynamics of a neuron in the inhibitory population is given by

$$\tau\frac{dV_j}{dt}=-V_j(t)+I_j+G_{ei}(t)[V_e-V_j(t)]$$
$$+G_{ii}(t)[V_i-V_j(t)], \quad (2)$$

where $G_{ii}(t)$ and G_{ei} represent the interactions whithin the inhibitory population and from the excitatory population to the inhibitory one, respectively. If $V_j(t)$ reaches the threshold value θ then it is reset instantly to 0. The output of the neuron j during a given time interval $[t_1,t_2]$ is given by number of spikes during that interval, that will be denoted by $O_j(t_1,t_2)$.

The evolution of the synaptic conductances is given by

$$G_{ab}(t)=\frac{F_{ab}}{N_a}\sum_{j\in a}\sum_{t_j^{spikes}} g_a(t-t_j^{spikes}), \quad (3)$$

where $a,b=e$ or i, F_{ab} are the coupling constants, and $g_a(t)$ describes the time course of the interaction. We choose a difference of two exponentials:

$$g_e(t)=\frac{1}{\tau_1^e-\tau_2^e}[\exp(-t/\tau_1^e)-\exp(-t/\tau_2^e)]\Theta(t) \quad (4)$$

and

$$g_i(t)=\frac{1}{\tau_1^i-\tau_2^i}[\exp(-t/\tau_1^i)-\exp(-t/\tau_2^i)]\Theta(t), \quad (5)$$

where τ_1^e and τ_2^e represent the rise and decay time constants for the excitation, τ_1^i and τ_2^i are the rise and decay time constants for the inhibition, and Θ is the Heaviside function.

The dynamics of the target neuron is given by

$$\tau\frac{dV}{dt}=-V(t)+G(t)[V_e-V(t)] \quad (6)$$

with a prescription for resetting identical to the one introduced above. The synaptic conductance is given by

$$G(t)=w_{signal}\sum_k g_e(t-t_k^{signal})$$
$$+w_{noise}\sum_{j\in e}\sum_{t_j^{spikes}} g_e(t-t_j^{spikes}). \quad (7)$$

Therefore the target neuron is receiving spikes from all the neurons in the excitatory population and an additional periodic spike train. The spike times in this train are given by $t_k^{signal}=kT$, where T is the period of the signal.

III. SIMULATION RESULTS

The network dynamics, Eqs. (1), (2), and (3), was integrated using a consistent second-order Runge-Kutta algorithm [16]. The membrane time constant was chosen as $\tau=10$ msec. The reversal potentials for excitation and inhibition are $V_e=30$ mV and $V_i=-10$ mV, respectively. The threshold is $\theta=20$ mV above rest. The synaptic time constants are given by $\tau_1^e=1$ msec, $\tau_2^e=3$ msec, $\tau_1^i=1$ msec, $\tau_2^i=7$ msec. The bias currents I_j were chosen in such a way that in the absence of interaction each population had a uniform distribution of firing rates in the interval $[f_a-\delta_a/2,f_a+\delta_a/2](a=e,i)$. The time step was $\delta t=0.1$ msec and the network had 8000 excitatory neurons and 8000 inhibitory neurons. Comparisons with different sizes were performed in order to check finite size effects. The dynamics was simulated during 8 sec. for each set of parameters investigated. In all of the figures the error bars represent an average over five realizations.

The dynamics of the target neuron Eq. (6) is solved simultaneously with the network dynamics and its output is Fourier transformed in order to evaluate its power spectrum. The value of the peak at the frequency of the periodic train is identified as the signal S, and the background value is the noise N. The signal-to-noise-ratio R is defined in the standard way:

$$R=10\ \log_{10}\frac{S}{N}. \quad (8)$$

We now examine the relation between the signal-to-noise ratio and the dynamical state of the network. One of the most important properties that characterizes the dynamical state of the network is its synchrony strength. The synchrony can be measured using the method developed in [17–19]. The method is based on the idea that in a synchronous state the fluctuations of the average membrane potential will be of the same order as the fluctuations of the individual potentials, while in an asynchronous state they will be much smaller if the system is large. The average membrane potential at time t for a system of N neurons is

$$A_N(t)=\frac{1}{N}\sum_{j=1}^{N} V_j(t). \quad (9)$$

Its time fluctuations can be characterized by the variance

$$\Delta_N=\langle A_N(t)^2\rangle_t-\langle A_N(t)\rangle_t^2. \quad (10)$$

This variance is normalized to the population averaged variance of single cell activity,

$$\Delta=\frac{1}{N}\sum_{j=1}^{N}[\langle V_j(t)^2\rangle_t-\langle V_j(t)\rangle_t^2]. \quad (11)$$

The resulting synchrony parameter

$$\chi=\lim_{N\to\infty}\frac{\Delta_N}{\Delta} \quad (12)$$

lies comprised between 0 and 1, and measures the degree of coherence of the system in the infinite size limit. In particular, $\chi=1$ if the system is totally synchronized [i.e., $V_j(t)=V(t)$ for all j] and $\chi=0$ if the state of the system is asynchronous. This quantity can be evaluated independently for both populations, giving rise to χ_e for the excitatory neurons and χ_i for the inhibitory ones.

Another important feature of the dynamical state is given by the possible existence of oscillations. It is important to stress that the question of oscillations is not independent of

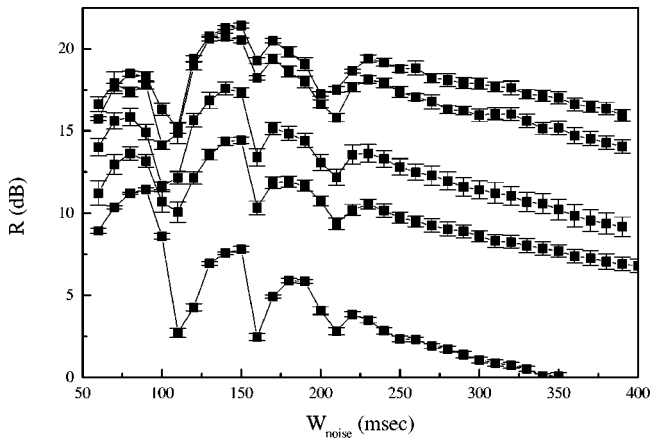

FIG. 1. Signal-to-noise ratio as a function of w_{noise} for $\delta_e=\delta_i=23,22,21,20,19$ Hz (from top to bottom). The value of the coupling constants is $F_{ee}=11$ msec, $F_{ei}=10$ msec, $F_{ie}=11$ msec, and $F_{ii}=10$ msec. The average firing rate of the excitatory population is approximately 54 Hz and the synchrony parameter χ_e takes the values 0.104, 0.124, 0.132, 0.136, and 0.137.

the synchrony. In an asynchronous state every neuron of a large system receives an input that is constant in time (up to corrections of order $1/\sqrt{N}$). An IF neuron that receives a constant input can have only two possible states: quiescent if the input is below threshold or periodic oscillations if it is above threshold. Therefore a nonzero degree of coherence is necessary to observe nonoscillatory behavior. This is not the case for the model studied in [13], where a neuron receiving a constant input can display chaotic behavior. On the other hand, when there is certain degree of coherence it is still possible to have oscillations, in particular, synchronized oscillations, besides the chaotic states.

The synchrony strength depends on all the parameters of the network (couplings, synaptic time constants, average firing rates, dispersion of firing rates) in a complex way. One case in which the relation is simpler is obtained by keeping all the parameters constant except for the dispersion of the firing rates δ_e and δ_i. In this case the synchrony is a monotonously decreasing function of the dispersions. In Fig. 1 we show the signal-to-noise ratio as a function of w_{noise} for different values of the dispersion: $\delta_e=\delta_i=23,22,21,20,19$ Hz. The strength of periodic signal was kept fixed at $w_{signal}=50$ msec. We can see that the signal-to-noise ratio is a *decreasing* function of the synchrony. Another interesting feature is the existence of multiple peaks in the signal-to-noise ratio. The existence of multiple peaks has been reported previously [20]. They are due to the presence of correlations in the noisy part of the input. In order to confirm this point in the present case we evaluate the probability density function of the network activity and generate a noise input with the same probability density function but without temporal correlations. In Fig. 2 we can see the probability density function of the network activity for $\delta_e=\delta_i=20$ Hz where the network activity at time t is defined by $O(t)=(1/N_e)\Sigma_{j\in e}O_j(t,t+\delta t)$. Using this density function to generate uncorrelated noise as input, the resulting signal-to-noise ratio is shown in Fig. 3. In the same figure we also show the result of using Gaussian white noise with a mean value and a dispersion obtained from the probability density

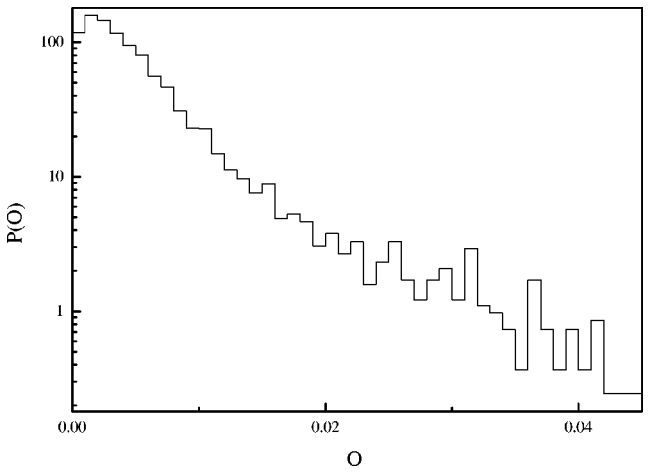

FIG. 2. Probability density function of the excitatory subnetwork activity O. The couplings are the same as in the previous figure and the disorder is $\delta_e=\delta_i=20$ Hz.

function of Fig. 2. Both instances of uncorrelated noise show a very similar behavior, and one which is very different from the noise generated by a network.

This result confirms the relevance of time correlations for stochastic resonance. In our case these temporal correlations are generated by a synchronized quasiperiodic component in the network activity, as can be seen in one example of the autocorrelation function of the network activity [see Fig. 4(a)]. By analyzing different network sizes and simulations times, we have checked that the peaks in the autocorrelation function are neither a finite size effect nor a transient effect. The power spectrum of the target neuron activity is shown in Fig. 5(a) for the same set of parameters. We can appreciate how clearly coherent peaks with the frequency of the signal and its harmonics emerge out of the broadband noise background.

For different network parameters the signal-to-noise ratio can be improved. We have changed the coupling parameters F_{ab} in order to find a state with less oscillations in the mean activity. In Fig. 6 we show the signal-to-noise ratio and its

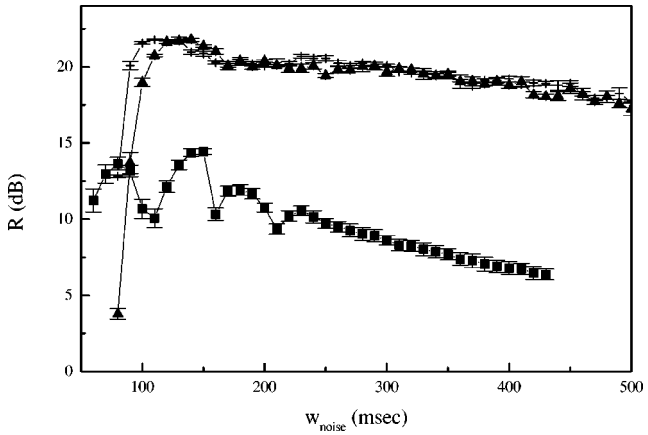

FIG. 3. Signal-to-noise ratio as a function of w_{noise}. Squares: noise generated by a network ($\delta_e=\delta_i=20$ Hz, $F_{ee}=11$ msec, $F_{ei}=10$ msec, $F_{ie}=11$ msec, and $F_{ii}=10$ msec). Crosses: white noise with the distribution of Fig. 2. Triangles: Gaussian white noise, with the mean value and dispersion of the probability density function of Fig. 2.

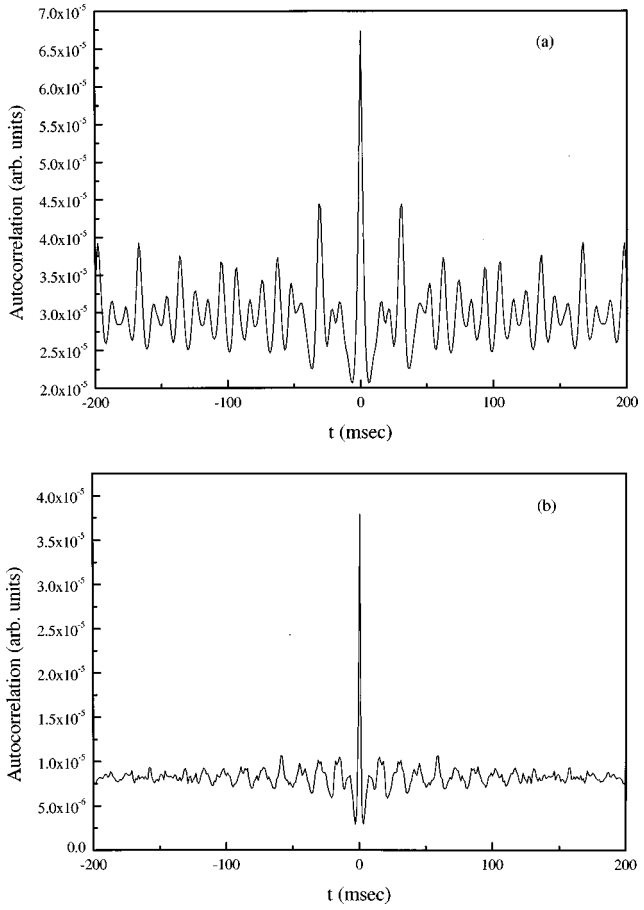

FIG. 4. Autocorrelation of the network activity $O(t)$. (a) $\delta_e = \delta_i = 20$ Hz, $F_{ee} = 11$ msec, $F_{ei} = 10$ msec, $F_{ie} = 11$ msec, and $F_{ii} = 10$ msec. (b) $\delta_e = \delta_i = 18$ Hz, $F_{ee} = 20$ msec, $F_{ei} = 22$ msec, $F_{ie} = 22$ msec, and $F_{ii} = 22$ msec.

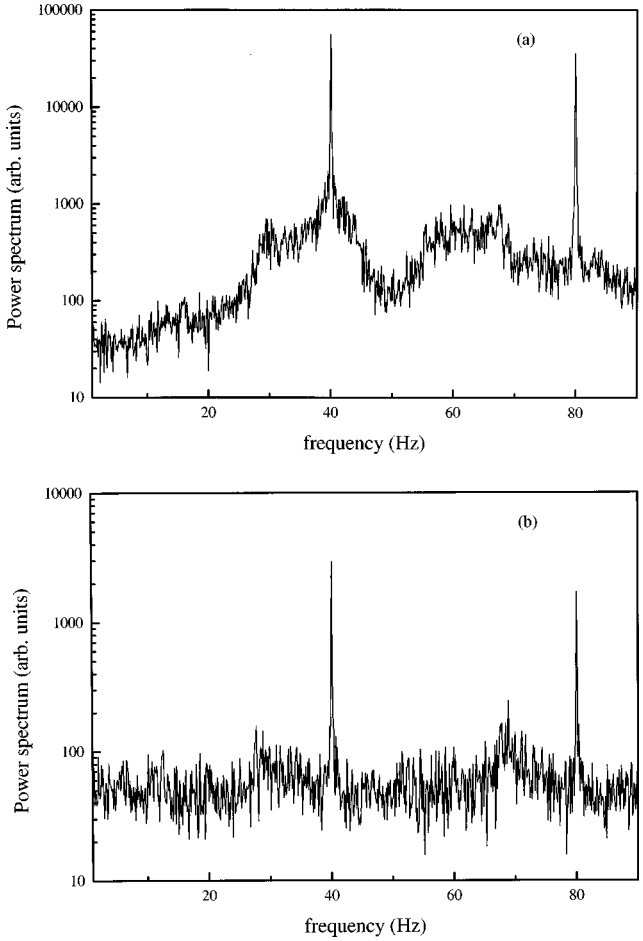

FIG. 5. Power spectrum of the target neuron activity. The periodic signal has a frequency of 40 Hz. (a) $\delta_e = \delta_i = 20$ Hz, $F_{ee} = 11$ msec, $F_{ei} = 10$ msec, $F_{ie} = 11$ msec, and $F_{ii} = 10$ msec (b) $\delta_e = \delta_i = 18$ Hz, $F_{ee} = 20$ msec, $F_{ei} = 22$ msec, $F_{ie} = 22$ msec, and $F_{ii} = 22$ msec.

comparison with noise generated with the probability density function of the network activity but without temporal correlations and with white Gaussian noise. The autocorrelation is shown in Fig. 4(b) and the power spectrum of the target neuron in Fig. 5(b). Although the autocorrelation is not completely flat it does not display such a strong long-term oscillatory component as in the previous case. This flatter spectrum generates a signal-to-noise ratio very similar to those of white noise. It is important to note that it is not necessary to fine tune all of the couplings to obtain this result. A change in one of them can be compensated by a change of the others, as long as the modification is not too large (approximately 20%).

In the simulations performed to obtain Figs. 1, 3, and 6 the firing rate of the target neuron is a monotonically increasing function of the noise strength, w_{noise}. In each case, its maximum value was chosen in such a way that the firing rate of the target neuron reached a maximum value of about 300 Hz. We found that the peak of the signal-to-noise ratio is reached for a firing rate of about 50–100 Hz (a similar value was found for the most sensitive range for signal transduction in a different model [21]). It is remarkable that the rate of decay of the signal-to-noise ratio is quite slow, especially in the case of Fig. 5, where in the whole range of w_{noise} from 200 to 600 msec, the firing rates changes by a factor of 5 but the signal-to-noise ratio decreases by less than 10%. This indicates that there is no need of fine tuning for w_{noise}.

IV. DISCUSSION

In this work we have analyzed the phenomenon of SR when the noise is generated by a network of interconnected IF neurons. Although we have not performed an exhaustive analysis of the network parameter space we can conclude that the temporal correlations of the output are a very important aspect of the dynamical state. This is demonstrated by the fact that using white noise with the same probability density function of the noise source but without temporal correlations we obtain very different values of the signal-to-noise ratio. Moreover, white noise eliminates multiple peaks in the signal-to-noise ratio as a function of noise intensity (see Fig. 3). Multiple peaks have also been observed in [22], but in this case they are not generated by temporal correlations in the noise, but by a scaling relation in the dynamical equations. Note that in this case the peaks appear evenly separated when plotted as a function of the logarithm of the noise intensity, while in our case the signal-to-noise ratio is plotted on a linear scale of the noise intensity. The influence of temporal correlations on SR has also been analyzed in

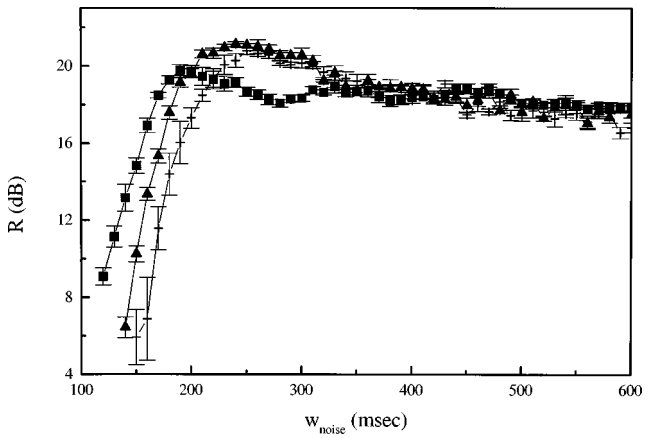

FIG. 6. Signal-to-noise ratio as a function of w_{noise}. Squares: noise generated by a network ($\delta_e = \delta_i = 18$ Hz, $F_{ee} = 20$ msec, $F_{ei} = 22$ msec, $F_{ie} = 22$, msec, and $F_{ii} = 22$ msec). The average firing rate and synchrony parameter χ for the excitatory (inhibitory) population are 28 Hz (40 Hz) and 0.07 (0.04). Crosses: white noise with the distribution of output network activity corresponding to the same parameters. Triangles: Gaussian white noise, with the mean value and dispersion of the probability density function of the corresponding output activity.

[23]. It was found that different sources of colored noise gave rise to different behaviors. In overdamped systems driven by colored noise SR is suppressed with increasing noise color. The opposite is found for colored noise induced by inertia, but it was never found the appearence of multiple peaks in the curve SR as a function of noise strength.

We have also observed that increasing the strength of synchrony by decreasing the dispersion of intrinsic frequencies leads to a decreasing signal-to-noise ratio. The reason for this behavior is that as synchrony increases the output becomes concentrated during short time intervals. Inside these intervals the noisy input is very strong and the output will be only weakly correlated with the signal while outside the intervals the signal is unable to generate any output.

These results suggest that the network parameters can be chosen in such a way that the detectability of weak signals is optimal. This will happen when the temporal correlations are small and the synchrony is not too strong. We expect that the relation between the dynamical states and the stochastic resonance must be qualitatively valid for models different from IF (for instance conductance based models) because, as it was shown in [20] in a simple case, the effect of the correlations in the noisy part of the input can be taken into account by using a probabilistic description of the system, that is independent on the details of the dynamics.

ACKNOWLEDGMENTS

We thank V. Grunfeld, H. Wio, and D. Zanette for a critical reading of the manuscript. This work was partially supported by CONICET through Grant No. PIP 4953/96, by ANPCyT through Grant No. PICT 97 03-00000-00131, and by CEB, Bariloche.

[1] C. Nicolis, Tellus **34**, 1 (1982).
[2] R. Benzi, G. Parisi, A. Sutera, and A. Vulpiani, Tellus **34**, 10 (1982).
[3] K. Wiesenfeld and F. Moss, Nature (London) **373**, 33 (1995).
[4] Author(s), in *Proceedings of the NATO Advanced Research Workshop on Stochastic Resonances in Physics and Biology*, edited by F. Moss, A. Bulsara, and M. F. Shlesinger, [J. Stat. Phys. **70**, 1 (1993)].
[5] N. G. Stocks, N. D. Stein, and P. V. E. McClintock, J. Phys. A **28**, L385 (1993).
[6] A. R. Bulsara, S. B. Lowen, and C. D. Rees, Phys. Rev. E **49**, 4989 (1994).
[7] X. Godivier and F. Chapeau-Blondeau, Europhys. Lett. **35**, 473 (1996).
[8] M. Riani and E. Siminotto, Phys. Rev. Lett. **72**, 3120 (1994).
[9] J. K. Douglass, L. Wilkens, E. Pantazelou, and F. Moss, Nature (London) **365**, 337 (1996).
[10] J. J. Collins, T. T. Imhiff, and P. Grigg, J. Neurophysiol. **76**, 642 (1996).
[11] B. J. Gluckman, T. I. Netoff, E. J. Neel, W. L. Ditto, M. L. Spano, and S. J. Schiff, Phys. Rev. Lett. **77**, 4098 (1996).
[12] W. R. Softky and C. Koch, Neural Comput. **4**, 643 (1992).
[13] W. Wang and Z. D. Wang, Phys. Rev. E **55**, 7379 (1997).
[14] E. Pantazelou, C. Dames, F. Moss, J. Douglass, and L. A. Wilkens, Int. J. Bifurcation Chaos Appl. Sci. Eng. **5**, 101 (1995).
[15] H. C. Tuckwell, *Introduction to Theoretical Neurobiology* (Cambridge University Press, Cambridge, 1988).
[16] D. Hansel, G. Mato, C. Meunier, and L. Neltner, Neural Comput. **10**, 467 (1998).
[17] D. Hansel and H. Sompolinsky, Phys. Rev. Lett. **68**, 718 (1992).
[18] D. Golomb and J. Rinzel, Physica D **72**, 259 (1994).
[19] I. Ginzburg and H. Sompolinsky, Phys. Rev. E **50**, 3171 (1994).
[20] G. Mato, Phys. Rev. E **58**, 876 (1998).
[21] W. Wang, Y. Wang, and Z. D. Wang, Phys. Rev. E **57**, R2527 (1998).
[22] J. M. G. Vilar and J. M. Rubi, Phys. Rev. Lett. **78**, 2882 (1997).
[23] P. Hänggi, P. Jung, C. Zerbe, and F. Moss, J. Stat. Phys. **70**, 25 (1993).